

## **Evaluation of deformed image-based dose calculations for adaptive radiotherapy of nasopharyngeal carcinoma**

POON, Miranda, HOLBORN, Catherine <<http://orcid.org/0000-0002-2211-1022>>, CHENG, Ka Fai, FUNG, Winky Wing Ki and CHIU, George

Available from Sheffield Hallam University Research Archive (SHURA) at:

<https://shura.shu.ac.uk/16561/>

---

This document is the Accepted Version [AM]

### **Citation:**

POON, Miranda, HOLBORN, Catherine, CHENG, Ka Fai, FUNG, Winky Wing Ki and CHIU, George (2017). Evaluation of deformed image-based dose calculations for adaptive radiotherapy of nasopharyngeal carcinoma. Medical dosimetry : official journal of the American Association of Medical Dosimetrists. [Article]

---

### **Copyright and re-use policy**

See <http://shura.shu.ac.uk/information.html>

# **Evaluation of deformed image-based dose calculations for adaptive radiotherapy of nasopharyngeal carcinoma**

Miranda Poon, M.Sc.,\* Catherine Holborn, M.Sc.,<sup>†</sup> Ka Fai Cheng, M.Sc.,\* Winky Wing Ki Fung, M.Phil.,\* and George Chiu, D.H.Sc.\*

*\*Department of Radiotherapy, Hong Kong Sanatorium & Hospital, Hong Kong; and*

*<sup>†</sup>Sheffield Hallam University, Sheffield, United Kingdom*

Corresponding author: Miranda Poon, M.Sc., Department of Radiotherapy, Hong Kong Sanatorium & Hospital, G/F, Li Shu Pui Block, 2 Village Road, Happy Valley, Hong Kong. Tel: (+852) 2835-8916; Fax (+852) 2892-7509; E-mail: miranda.sw.poon@hksh.com

Conflict of interest: none.

Presented at the American Society for Radiation Oncology (ASTRO), 56<sup>th</sup> Annual Meeting, San Francisco, CA, September 17, 2014.

This research did not receive any specific grant from funding agencies in the public, commercial, or not-for-profit sectors.

## **Abstract**

### **Purpose:**

To evaluate the dosimetric accuracy of using deformed CT images for dose calculations, and to assess the feasibility of using these images during adaptive radiotherapy, for nasopharyngeal carcinoma (NPC) patients.

### **Methods and Materials:**

Thirty consecutive NPC patients who had undergone one re-plan in their radiotherapy treatments were selected. The pre-treatment planning computed tomography (PCT) images were deformed to match the mid-treatment PCT images by deformable image registration. The same volumetric modulated arc therapy plan was then calculated on the deformed PCT images. The resulting dose distributions and dose volume histograms of the tumours and organs at risk (OARs) were compared to the original plan. Five dose levels including  $D_{98\%}$ ,  $D_{95\%}$ ,  $D_{50\%}$ ,  $D_{5\%}$ , and  $D_{2\%}$  were recorded for 9 NPC targets. Four dose levels including  $D_{\max}$ ,  $D_{10\%}$ ,  $D_{50\%}$ , and  $D_{\text{mean}}$  were recorded for 15 OARs.

### **Results:**

The greatest percentage difference in observed dose for  $D_{98\%}$ ,  $D_{95\%}$ ,  $D_{50\%}$ ,  $D_{5\%}$ , and  $D_{2\%}$  of the targets were 1.71%, 1.55%, 0.64%, 0.97%, and 1.13%, respectively. The greatest percentage difference in observed dose for  $D_{\max}$ ,  $D_{10\%}$ ,  $D_{50\%}$ , and  $D_{\text{mean}}$  of the OARs were -26.51% (left optic nerve), -17.06% (left optic nerve), 56.70% (spinal cord), and 18.97% (spinal cord), respectively. In addition, 29 out of 45 (64%) dosimetric endpoints of the targets showed statistically significant dose differences ( $P < 0.05$ ) between the original plan and the plan calculated on deformed images. Forty-nine out of 60 (82%) dosimetric endpoints of the OARs also showed statistically significant dose differences

( $P < 0.05$ ).

**Conclusions:**

Dose calculations using deformed PCT images could result in significant dose uncertainties for NPC patients. Further investigations are needed; meanwhile, it is suggested that a new PCT should be acquired in the case of re-planning at mid-course.

**Keywords:** Nasopharyngeal carcinoma; Deformable image registration; Adaptive radiation therapy; Dose calculation; Treatment planning

## Introduction

Adaptive radiotherapy (ART) is a novel approach to correct for tumour and normal tissue variations during the course of treatment in order to maintain optimal target dose coverage and critical organs sparing. This approach, however, will require additional computed tomography (CT) acquisitions which will increase workloads to the department and radiation dose to the patient. The use of on-treatment cone-beam CT (CBCT) images for the purposes of re-planning can avoid extra CT acquisitions but may not be feasible for contour delineations and dose calculations due to their relatively poor image quality (1). An ideal alternative would be the use of deformable image registration (DIR) to deform the planning CT (PCT) images to up-to-date CBCT images for dose calculations.

In this study, phase I (Ph I) PCT images were deformably registered to match the anatomy at phase II (Ph II) PCT images. The rationale for not using CBCT images to perform the DIR was because the PCT-CBCT registration error could be a potential confounding variable. A CT-CBCT registration is known as a quasi-intermodality case and Zhen *et al.* acknowledged the fact that there are uncertainties and errors existing in such DIR (2). Although the underlying physical acquisition process for the CT and CBCT images is identical, the acquisition geometry is different which causes the CBCT to be corrupted by noise and artefacts (3). The purpose of this study was to first evaluate the accuracy of using a CT-CT DIR (i.e. images of same modality) for dose calculations so that the result could then determine whether further study on the accuracy of using CT-CBCT DIR for dose calculations is needed.

## Methods and Materials

### *Patient population, image registration and treatment planning*

Thirty consecutive nasopharyngeal carcinoma (NPC) patients who had completed their radiotherapy treatment to the nasopharyngeal region and the bilateral lymph nodes

between 2010 and 2013 were retrospectively selected. These patients must have received 2-phase radiotherapy treatment which included a mid-course PCT scan. Any patients with CT images that had substantial artefacts such as numerous dental fillings, were excluded.

Helical PCTs were acquired using GE LightSpeed CT-simulator (GE Healthcare Technologies, Milwaukee, WI) at a 2.5-mm slice thickness. The Ph II PCT scans were acquired between the 6th to 20th fraction of their treatment. The number of days between Ph I and II PCT took place ranged from 25 to 63 days. The Ph I and II image sets were deformably registered using a commercially available image registration software, MIM Maestro version 6.1.1 (MIM Software, Cleveland, OH). The deformation engine applies a constrained intensity-based free-form deformable registration algorithm for CT-CT registration (4). Image registrations were performed by the same investigator on a desktop computer with an Intel® Xeon® Processor W3550 at 3.07 GHz and a 12.0 GB RAM.

All dose calculations were performed using Eclipse v10.0 (Varian Medical Systems, Palo Alto, CA) with a calculation grid size of 0.25cm. The calculation algorithm used was the Varian Anisotropic Analytical Algorithm model version 10.0.28.

### *Workflow and methodology*

The workflow and methodology are presented in Fig. 1. Group I represents the normal route through which patients had undergone one replan during the course of their treatment. Group II consists of the same patients as in group I and each patient's Ph II PCT was used as a reference image to which the Ph I PCT was registered. Initially the CT images were co-registered using a rigid automatic match tool followed by some manual adjustments, mainly based on the nasopharyngeal region, in order to optimise the alignment to the primary tumour. The deformable registration algorithm was then applied.

The deformable alignment accuracy was tested based on a few manually identified landmarks. The same 6 MV volumetric modulated arc therapy (VMAT) plan was applied and re-calculated on the deformed PCT images. The treatment plans in group I and II for each patient were examined and compared dosimetrically.

### *Plan comparison*

Two dose volume histograms (DVHs) and isodose distributions were generated for each patient based on Ph II PCT and deformed PCT. The dose tolerances for various OARs according to QUANTEC (5-10) were recorded and compared. The treatment plan comparisons were done in three approaches:

#### 1) Dose patterns in target volumes

There were 9 targets for each patient, namely NP-GTV, NP-CTV, NP-PTV, left/right LN-GTV, left/right LN-CTV and left/right LN-PTV. The term “NP”, “LN”, “GTV”, “CTV”, and “PTV” represent the nasopharyngeal region or the primary tumour, the bilateral lymph nodes, the gross tumour volume, the clinical target volume, and the planning target volume, respectively. Five dose levels,  $D_{98\%}$ ,  $D_{95\%}$ ,  $D_{50\%}$ ,  $D_{5\%}$  and  $D_{2\%}$ , were recorded for each curve. Percentage differences were calculated as  $100 \times ((B-A)/A)$ , where B and A were the doses calculated based on deformed PCT and Ph II PCT, respectively.

#### 2) Dose patterns in organs at risk (OARs)

Four dose levels, i.e.  $D_{\max}$ ,  $D_{10\%}$ ,  $D_{50\%}$  and  $D_{\text{mean}}$  were recorded for 15 OARs. The 15 OARs were brainstem, spinal cord, left/right eyes, left/right lens, left/right cochleas, optic chiasm, left/right optic nerves, oral cavity, larynx, and left/right parotid glands. Percentage differences were also calculated.

### 3) DVHs and isodose distributions comparison

DVH comparison was performed between the original plan generated from Ph II PCT and the new plan generated from the deformed PCT. Isodose distributions were also compared visually for individual patients.

#### *Statistical analysis*

The statistical test used was the two-tailed paired t-test for the normally distributed data and the Wilcoxon signed-rank test for the non-normally distributed data. A  $p$ -value of  $<0.05$  was considered statistically significant. GraphPad Prism version 5.0c for Mac OS X (GraphPad Software, San Diego, CA) was used for statistical analysis. The null hypothesis of the study was that there is no difference between the two groups.

## **Results**

#### *Target volumes dose comparison*

Table 1 (top) summarises the dose statistics analysis of the pairwise comparison between the dose calculations using conventional PCT and deformed PCT images for the target volumes. For simplicity, only the greatest percentage differences within the dose level for each nasopharyngeal target volume are shown. Twenty nine out of 45 (64%) dosimetric endpoints of the target volumes showed statistically significant dose differences ( $p<0.05$ ) between the two groups. The greatest percentage difference in observed dose for  $D_{98\%}$ ,  $D_{95\%}$ ,  $D_{50\%}$ ,  $D_{5\%}$ , and  $D_{2\%}$  of the target volumes were 1.71% (right LN-GTV), 1.55% (right LN-GTV), 0.64% (right LN-GTV), 0.97% (NP-GTV), and 1.13% (NP-GTV and NP-CTV), respectively.

#### *OARs dose comparison*

The dose statistics analysis of the pairwise comparison for spinal cord, left and right



optic nerves is shown in table 1 (bottom) as the greatest differences were observed in these OARs. As with the target volumes, only the greatest percentage differences within the dose level for the OARs are shown for simplicity. Forty-nine out of 60 (82%) dosimetric endpoints of the OARs showed statistically significant dose differences ( $p<0.05$ ) between the two groups. The greatest percentage difference in observed dose for  $D_{\max}$ ,  $D_{10\%}$ ,  $D_{50\%}$ , and  $D_{\text{mean}}$  of the 15 OARs were -26.51% (left optic nerve), -17.06% (left optic nerve), 56.70% (spinal cord), and 18.97% (spinal cord), respectively. For left optic nerve, the mean percentage difference in observed dose for  $D_{\max}$  and  $D_{10\%}$  were -4.57% (SD=5.77) and -3.52% (SD=3.66). For spinal cord, the mean percentage difference in observed dose for  $D_{50\%}$  and  $D_{\text{mean}}$  were 3.70% (SD=10.56) and 2.79% (SD=5.00).

Table 2 shows the patient specific dose differences for spinal cord and left optic nerve. Deviations of more than 5% can be observed in 3 OARs including brainstem, right cochlea and right eye. Deviations of more than 10% can be observed in right lens. Deviations of more than 15% can be observed in 5 OARs including spinal cord, left lens, optic chiasm, left optic nerve and right optic nerve.

### *Example of individual results*

Figures 2A, 3A and 4A show the registration result and dosimetric comparison of a NPC patient with Stage III T2bN2M0 undifferentiated carcinoma. Good agreement was found between the Ph II PCT (solid line) and the deformed PCT (dotted line) based dose calculations for the target volumes and OARs (Fig. 2A). Only minimal anatomical changes were observed on the Ph II PCT as compared with Ph I PCT (Fig. 3A). The overall isodose distributions on the Ph II PCT scan (left) and the deformed PCT scan (right) were quite comparable (Fig. 4A).

Figures 2B, 3B, and 4B show the results of another NPC patient with Stage III T1N2M0 undifferentiated carcinoma. There were dose discrepancies between the Ph II

PCT (solid line) and deformed PCT (dotted line) calculations for OARs including left lens (yellow), left optic nerve (light blue), right optic nerve (dark purple), and spinal cord (cyan) (Fig. 2B). The largest discrepancy was observed in spinal cord in particular. Rigid registration result shows a relatively better alignment in the nasopharyngeal region at the level of base of skull and C1 vertebra, however, a significant mismatch was seen in the neck region starting from C5 vertebra and below (Fig. 3B). Despite the mismatch at the neck region, isodose distributions in the level of C5 vertebra were quite comparable (Fig. 4B).

Figures 2C, 3C, and 4C show the results of a patient with a primary tumour that was in close proximity to the optic chiasm and the optic nerves. The rigid registration result was excellent (Fig. 3C), however, there was a significant dosimetric discrepancy between the DVHs for left (light blue) and right (dark purple) optic nerves (Fig. 2C). In addition, a difference in isodose distributions especially in the air cavity-soft tissue interface around the paranasal sinuses can be observed (Fig. 4C).

## Discussion

Re-plans are common encounters in radiotherapy of NPC patients due to tumour or normal tissue changes during the course of treatment. Acquiring a new PCT for re-planning causes extra radiation exposure to the patient and increases workload to the radiation department. One method that is being widely investigated to replace the need of acquiring new PCT is to use the on-treatment kV CBCT images for dose calculation (1, 11-14).

Yang *et al.* and Yadav *et al.* both studied the accuracy of CBCT-based dose calculation with the intention of determining the feasibility of using these images for the purpose of dosimetric checks (1, 13). Their results showed that it is acceptable to use CBCT images for dose calculation. Two studies, one by Ding *et al.* and the other by Hu

*et al.*, further investigated the feasibility of using CBCT for treatment planning in ART (11, 14). Their results were also in good agreement that CBCT-based treatment plans were dosimetrically comparable to CT-based treatment plans. Although the results sounded promising, the authors of both studies suggested that CBCT images should only be used for dosimetric validation at the moment. An additional PCT will still be necessary to perform re-planning because of the suboptimal image quality of CBCT. The inferior image quality of CBCT due to scattered radiation may hinder the oncologist's ability to accurately delineate the tumour and critical organs. In addition, the slow gantry rotation speed of the linac makes the CBCT more prone to motion artefacts (1). Another limitation of CBCT is the limited field of view (especially in the longitudinal direction) which renders the resultant images non-usable for treatment planning (14). Given these limitations, our study explored the possibility of using a deformed CT image for dose calculations in order that up-to-date tumour and normal tissue information can be used for treatment planning without acquiring a new PCT while maintaining acceptable image quality for accurate delineation.

The results of this study, however, demonstrated that treatment planning with deformed PCT images may lead to dosimetric uncertainties. Target dose comparison shows better agreement, when compared to OARs dose comparison, in dosimetric difference between conventional PCT-based treatment plans and deformed PCT-based treatment plans. Although statistical significance was found in 64% of the target volume dosimetric endpoints, the greatest percentage difference was only 1.71% which may not necessarily be clinically significant. The DVHs for all the target volumes nearly overlay one another showing dosimetric consistency between the 2 CT scans (Fig. 2).

Larger dose discrepancies, on the other hand, were seen in the OARs especially in critical structures such as the lens, optic chiasm, optic nerves and spinal cord. Eighty two percent of the dosimetric endpoints showed statistically significant difference. In addition,

dose differences that were greater than  $\pm 5\%$ ,  $\pm 10\%$ ,  $\pm 15\%$ , and up to 56.7%, can be observed in the OARs dose comparisons. Such large dose deviations could translate into significant clinical outcomes which adversely affect the intention of ART.

Individual examples shown above suggested that the large dose deviation found may be due to residual registration error. Patient one (Fig. 2A, 3A, 4A) remained anatomically consistent throughout the treatment as an excellent rigid registration result was obtained, even though the time frame between Ph I and Ph II PCT was 25 days apart. The resulting DVHs and isodose distributions both demonstrated excellent agreement between the conventional PCT-based and deformed PCT-based treatment plans. Patient two (Fig. 2B, 3B, 4B) experienced a change in anatomical structures between the Ph I and II PCT which could be caused by setup reproducibility error or a change in patient's body weight. The decision to align the CT images based on the base of skull, nasopharyngeal region and C1-2 vertebra was made because it was believed that priority should be given to maintaining a good alignment around the primary tumour area, hence a resulting mismatch of the C5 vertebra and the region below was inevitable. The suboptimal result of the rigid registration may lead to a residual error in deformable registration. The resulting large dose deviation seen in the DVHs of the spinal cord subsequently confirmed the speculation of residual registration error. Despite the large dose deviation on the DVHs, it was difficult to identify the difference in isodose distribution (Fig. 4A). Patient three (Fig. 2C, 3C, 4C) showed large dose discrepancies for the optic nerves between conventional CT-based and deformed CT-based treatment plans. Accuracy in dose calculation is particularly essential in this patient to ensure the dose received by the optic nerves stayed within tolerance. The isodose distribution demonstrated a significant difference especially in the air-tissue interface in the paranasal sinus region (Fig. 4C). Despite a satisfactory result in the alignment of the bony anatomy (Fig. 3C), the dose discrepancies shown in this case suggested that deformable registration result may be

unreliable for structures that are small with lack of contrast with the background. This was further confirmed by the results in which large dose deviations were generally observed in smaller OARs such as the lens, eyes, optic nerves, optic chiasm and cochleas. When the dose to the OARs are reaching tolerance limits such as in cases when the tumour is extremely close to structures like brainstem or optic nerves, or in cases when the patient is having another course of radiation treatment due to local recurrence, any deviations in dose calculation accuracy may lead to serious consequences. The results in this study, therefore, suggested that the deformed image-based dose calculation will create dose uncertainties that may not be suitable for re-plan in NPC patients.

As mentioned earlier, the PCT-CBCT registration may introduce image noise and produce registration results that were less accurate. The results presented here suggested that the use of CT-CT DIR failed to provide accurate dose calculations which further suggest that a PCT-CBCT DIR may produce equal or even less accurate results. One limitation of this study was that the assessment of DIR accuracy was difficult. Although inter-observer variation was avoided by performing all registration procedures by a single investigator, the accuracy of the deformable registration was still difficult to quantify. One approach used in this study was manually identifying several critical anatomical landmarks for verification by visual inspection, however, it may not be sufficient for generalising the accuracy results to the entire region of interest. In addition, when there is a significant change in anatomy between the 2 image sets as encountered in patient two, how the rigid registration was performed became a subjective decision by the individual investigator. No consensus guidelines exist on whether matching to several important structures is more desirable than matching to the overall trend. Kashani *et al.* found that different implementations, different users, or different parameter settings of the same type of registration can result in different accuracy (15). Accomplishing deformable registration with accuracy is particularly essential in this study because precise ART

cannot be delivered if there are registration errors which would defeat the purpose of the re-plan.

In this study, a commercially available image registration software was used which utilises a constrained intensity-based free-form deformable registration algorithm for CT-CT registration. A more robust DIR algorithm is desirable in order to increase the accuracy. Several techniques have been used to accomplish accurate DIR (2, 16-17). Castadot *et al.* compared 12 DIR strategies for the treatment of head and neck tumours (16). Their results show that the use of the Demons' algorithm, implemented in multi-resolution, followed by the level-set algorithm and using images that have undergone preliminary edge-preserving denoising, is a good registration strategy for head and neck ART. The full explanation of the technical details of this method can be found in the original paper. Zhen *et al.* also suggested that the use of Demons algorithm for CT-CT registration and a modified demons algorithm known as Deformation with Intensity Simultaneously Corrected (DISC) for CT-CBCT registration can produce a robust result (2).

## **Conclusions**

Future investigation using a more robust DIR algorithm may lead to more accurate dose calculation results. It is important to evaluate the dosimetric accuracy of using deformed image for dose calculations because it could potentially replace the need of re-plan CT, and as a result, reduce the radiation exposure of the patient and the workload of the department.

## References

1. Yang, Y.; Schreibmann, E.; Li, T.; *et al.* Evaluation of on-board kV cone beam CT (CBCT)-based dose calculation. *Phys. Med. Biol.* **52**:685-705; 2007.
2. Zhen, X.; Gu, X.; Yan, H.; *et al.* CT to cone-beam CT deformable registration with simultaneous intensity correction. *Phys. Med. Biol.* **57**:6807-26; 2012.
3. Lawson, J.D.; Schreibmann, E.; Jani, A.B.; *et al.* Quantitative evaluation of a cone-beam computed tomography-planning computed tomography deformable image registration method for adaptive radiation therapy. *J. Appl. Clin. Med. Phys.* **8**:96-113; 2007.
4. Piper, J.W. Evaluation of an intensity-based free-form deformable registration algorithm. *Med. Phys.* **34**:2353-4; 2007.
5. Mayo, C.M.; Martel, M.K.; Marks, L.B.; *et al.* Radiation dose-volume effects of optic nerves and chiasm. *Int. J. Radiat. Oncol. Biol. Phys.* **76**(suppl.):28-35; 2010.
6. Mayo, C.M.; Yorke, E.; Merchant, T.E. Radiation associated brainstem injury. *Int. J. Radiat. Oncol. Biol. Phys.* **76**(suppl.):36-41; 2010.
7. Kirkpatrick, J.P.; van der Kogel, A.J.; Schultheiss, T.E. Radiation dose-volume effects in the spinal cord. *Int. J. Radiat. Oncol. Biol. Phys.* **76**(suppl.):42-9; 2010.
8. Bhandare, N.; Jackson, A.; Eisbruch, A.; *et al.* Radiation therapy and hearing loss. *Int. J. Radiat. Oncol. Biol. Phys.* **76**(suppl.):50-7; 2010.
9. Deasy, J.O.; Moiseenko, V.; Marks, L.; *et al.* Radiotherapy dose-volume effects on salivary gland function. *Int. J. Radiat. Oncol. Biol. Phys.* **76**(suppl.):S58-63; 2010.
10. Rancati, T.; Schwarz, M.; Allen, A.M.; *et al.* Radiation dose-volume effects in the larynx and pharynx. *Int. J. Radiat. Oncol. Biol. Phys.* **76**(suppl.):64-9; 2010.
11. Ding, G.X.; Duggan, D.M.; Coffey, C.W.; *et al.* A study on adaptive IMRT treatment planning using kV cone-beam CT. *Radiother. Oncol.* **85**:116-25; 2007.
12. Yoo, S.; Yin, F.F. Dosimetric feasibility of cone-beam CT-based treatment planning

compared to CT-based treatment planning. *Int. J. Radiat. Oncol. Biol. Phys.* **66**:1553-61; 2006.

13. Yadav, P.; Ramasubramanian, V.; Paliwal, B.R. Feasibility study on effect and stability of adaptive radiotherapy on kilovoltage cone beam CT. *Radiol. Oncol.* **45**:220-6; 2011.
14. Hu, W.; Ye, J.; Wang, J.; *et al.* Use of kilovoltage X-ray volume imaging in patient dose calculation for head-and-neck and partial brain radiation therapy. *Radiol. Oncol.* **5**:29-38; 2010.
15. Kashani, R.; Hub, M.; Balter, J.M.; *et al.* Objective assessment of deformable image registration in radiotherapy: A multi-institution study. *Med. Phys.* **35**:5944-53; 2008.
16. Castadot, P.; Lee, J.A.; Parraga, A.; *et al.* Comparison of 12 deformable registration strategies in adaptive radiation therapy for the treatment of head and neck tumors. *Radiother. Oncol.* **89**:1-12; 2008.
17. Li, D.; Wang, H.; Yin, Y.; *et al.* Deformable registration using edge-preserving scale space for adaptive image-guided radiation therapy. *J. Appl. Clin. Med. Phys.* **12**:105-23; 2011.



## Figure Legends

Fig. 1. Workflow diagram illustrating different steps to obtain dose and volume parameters.

Table 1. Statistical analysis of the dosimetry differences between the treatment plans based on the deformed PCT images and the original PCT images for the nasopharyngeal target volumes (top) and OARs (bottom).

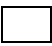



Table 2. Patient specific dose differences for spinal cord and left optic nerve. The “-”, “+” or “0” sign indicates that the dose calculated with the deformed PCT image is smaller than, larger than, or no differences with the dose calculated with the original PCT image, respectively.  difference within  $\pm 5\%$ ;  difference is greater than  $\pm 5\%$ ;  difference is greater than  $\pm 10\%$ ;  difference is greater than  $\pm 15\%$ .

Fig. 2A-C. DVHs comparison of target volumes and OARs for the treatment plans generated by the original PCT (solid line) and deformed PCT (dotted line) for (A) patient one; (B) patient two; and (C) patient three.

Fig. 3A-C. Rigid and deformable registration results for the three corresponding patients shown in fig. 2. The top panel shows the orthogonal views of the rigid registration with checkerboard overlay of the 2 CT scans and the bottom panel shows the orthogonal views of the CT image after deformable registration.

Fig. 4A-C. Isodose distributions comparison of CT-based (left) and deformed CT-based (right) VMAT plans for the three corresponding patients shown in fig. 2 and 3.